

Conductance anomalies in a normal-metal- d -wave superconductor junction

J. H. Xu, J. H. Miller, Jr., and C. S. Ting

Department of Physics and Texas Center for Superconductivity, University of Houston, Houston, Texas 77204

(Received 31 August 1994; revised manuscript received 21 February 1995)

The effects of Andreev reflection on the current-voltage characteristic and differential conductance of a junction between a normal metal and a d_{xy} -wave superconductor, or equivalently, a $d_{x^2-y^2}$ -wave superconductor with a $\{110\}$ -oriented surface are investigated using the Bogoliubov-de Gennes equations. Our study elucidates several important consequences of the sign change of a d -wave order parameter. In particular, a zero-bias conductance peak is obtained when an insulating barrier exists at the interface between the normal metal and the d -wave superconductor, consistent with numerous experiments performed on cuprate superconductors. If the insulating barrier is assumed to reside in the normal metal, several coherence lengths away from the superconductor surface, bound states within the energy gap, and consequent subgap resonances in the differential conductance, are predicted. The positions of these resonances are out of phase with respect to those predicted for an isotropic or anisotropic s -wave superconductor, thus providing unique signatures of pairing state symmetry.

I. INTRODUCTION

Recently, there has been considerable interest in the understanding of the pairing symmetry in high- T_c superconductors. Theoretical model studies¹ based on spin-fluctuation mediated pairing strongly suggest that the condensate of cuprate high- T_c superconductors might have $d_{x^2-y^2}$ -wave symmetry (defined relative to the a and b crystal axes of the CuO_2 planes). Such a pairing state gives rise to an anisotropic energy gap $\Delta(\mathbf{k}) = \Delta_0(\hat{k}_a^2 - \hat{k}_b^2)$, which reduces to zero along nodes of an essentially cylindrical Fermi surface, implying the existence of low-energy excitations. This is very different from the conventional BCS s -wave superconductors, which have a finite energy gap over the entire Fermi surface. This difference can result in very different temperature (T) dependences of numerous thermodynamic and transport properties, namely, power-law T dependence for d -wave superconductors versus exponentially activated behavior for s -wave superconductors. Experimentally, many measurements of such quantities on high- T_c materials indeed show power-law T dependences. For example, a linear- T dependence of the London penetration depth has been observed and interpreted by Hardy *et al.*² as an indication of d -wave superconductivity. Shen *et al.*³ have measured the angle-resolved photoemission spectrum of a single-crystal high- T_c superconductor, and the results indeed show an anisotropic energy gap, which also supports a d -wave pairing state. However, such interpretations are not unambiguous, since these experimental results depend only on a vanishing energy gap along certain directions in k space, and not on the sign or phase of the gap function. Thus, in principle, these experiments can also be interpreted in terms of an anisotropic s -wave pairing state, for example, $\Delta(\mathbf{k}) = \Delta_0|\hat{k}_a^2 - \hat{k}_b^2|$.

On the other hand, there exist a number of experiments designed to directly probe the sign change of a d -wave pairing state in high-temperature superconductors.⁴⁻⁷ Wollman *et al.*⁴ measured the field-modulated critical currents of cor-

ner superconducting quantum interference devices (SQUID's) and junctions, which combine an s -wave superconductor with a Y-Ba-Cu-O single crystal. Their results provide strong evidence for a π -phase shift in the Josephson coupling energy predicted for a d -wave pairing state. Mathai *et al.*⁵ performed a similar experiment on Y-Ba-Cu-O-Ag-Pb SQUID's using a scanning SQUID microscope, and they claimed that their results provide unambiguous evidence for a time-reversal invariant $d_{x^2-y^2}$ symmetric order parameter. Tsuei *et al.*⁶ used the concept of flux quantization in a tricrystal superconducting Y-Ba-Cu-O ring with grain-boundary Josephson junctions to determine the pairing symmetry. They observed spontaneous magnetization of half a flux quantum, consistent with d -wave pairing symmetry. Miller *et al.*⁷ proposed a new method of probing the pairing symmetry by measuring the field-modulated critical current of tricrystal devices. Their results in the short junction limit indicate a clear phase shift in the Josephson coupling, suggesting predominantly d -wave pairing symmetry. In short, these recent experiments that directly probe the pairing symmetry of high- T_c superconductors appear to favor a d -wave pairing state. It has also been suggested that a heavy-fermion superconductor, URu_2Si_2 with $T_c = 1.2$ K, might have a d -wave pairing state.^{8,9} Both point-contact and specific-heat measurements for URu_2Si_2 in the superconducting state are consistent with an energy gap that has d_{xy} -wave symmetry.

In this work, we examine another direct consequence of the sign change of a d -wave superconducting order parameter — namely, its effects on quasiparticle tunneling experiments. The current-voltage (I - V) characteristics will be studied for a normal metal- d_{xy} -wave superconductor junction (hereafter, we will call it a d_{xy} -NS junction, see Fig. 1). Such a d_{xy} -NS junction is formed as follows: for the heavy-fermion superconductor URu_2Si_2 with d_{xy} -wave symmetry, we choose a $\{100\}$ surface and a coordinate system (x, y, z) such that $x > 0$ is the region occupied by the superconductor. For high- T_c superconductors with $d_{x^2-y^2}$ -wave symmetry, we choose a $\{110\}$ surface and a new coordinate system (x, y, z) such that $x > 0$ is also the region occupied by the

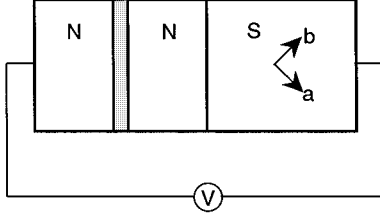


FIG. 1. A Schematic of a d_{xy} -NS junction formed by a $d_{x^2-y^2}$ -wave superconductor (S) with a $\{110\}$ surface. The shaded region corresponds to an insulating barrier inside the normal metal (N).

superconductor, and the z axis is still along the $[001]$ -crystal direction. In this fashion, a d_{xy} -NS junction can be formed by a superconductor with $d_{x^2-y^2}$ -wave symmetry (see Fig. 1). This study was originally motivated by the experimental observation of the so-called zero-bias anomaly (ZBA),¹¹ i.e., a peak in differential conductance that is often observed at zero-bias voltage in normal metal-high- T_c superconductor junctions, and by a recent theoretical work of Hu,¹² in which he predicted that a “midgap” state exists on the $\{110\}$ surface of a $d_{x^2-y^2}$ -wave superconductor. Reference 13 gives a comprehensive review on this subject. We show that there exist bound states within the gap which cause steps in the I - V characteristics and subgap resonances in the differential conductance. The positions of these current steps or resonances are out of phase relative to those obtained for conventional s -wave NS junctions. In particular, a zero-voltage step in the I - V curve, or a resonance corresponding to the ZBA in the conductance can also be obtained for the this junction.

In Sec. II, we present the Bogoliubov–de Gennes (BdG) equations¹⁴ for the inhomogeneous superconducting system with a d -wave order parameter. We show that the one-dimensional BdG equations can be solved exactly if the proximity effect is neglected. In Sec. III, we adopt the model and formalism of Blonder, Tinkham, and Klapwijk (BTK),¹⁵ and extend the calculation to the d_{xy} -NS junction. The possible correlation between our results and experiments will be discussed. Finally, in Sec. IV, a summary and discussion of our results will be given.

II. BDG EQUATIONS FOR A d -WAVE SUPERCONDUCTOR

In the BdG formalism, the quasiparticles in an inhomogeneous anisotropic d -wave superconducting system are represented by a two-element column vector ψ :

$$\psi(\mathbf{x}) = \begin{pmatrix} u(\mathbf{x}) \\ v(\mathbf{x}) \end{pmatrix}, \quad (2.1)$$

where $u(\mathbf{x})$ and $v(\mathbf{x})$ are the electron and hole components of the quasiparticle excitations, and obey the BdG equations

$$Eu(\mathbf{x}) = h_0 u(\mathbf{x}) + \int d\mathbf{x}' \Delta(\mathbf{x}, \mathbf{x}') v(\mathbf{x}'), \quad (2.2)$$

$$Ev(\mathbf{x}) = -h_0 v(\mathbf{x}) + \int d\mathbf{x}' \Delta(\mathbf{x}, \mathbf{x}') u(\mathbf{x}'), \quad (2.3)$$

where $h_0 = -\nabla^2/2m + V(\mathbf{x}) - \mu$ is the single-particle Hamiltonian with μ being the Fermi energy, $V(\mathbf{x})$ and $\Delta(\mathbf{x}, \mathbf{x}')$ are the ordinary potential and pair potential, respectively. Note that the dependence of $\Delta(\mathbf{x}, \mathbf{x}')$ on \mathbf{x} and \mathbf{x}' cannot be reduced to a dependence on the difference of the two coordinates as in the homogeneous case.¹⁶ However, the quantities that depend on \mathbf{x} and \mathbf{x}' can be written in terms of the center of mass $\mathbf{R} = (\mathbf{x} + \mathbf{x}')/2$ and the relative coordinate $\mathbf{r} = \mathbf{x} - \mathbf{x}'$. Namely, $\Delta(\mathbf{x}, \mathbf{x}') \equiv \Delta(\mathbf{r}, \mathbf{R})$. Then, after a Fourier transform with respect to \mathbf{r} , we have

$$\Delta(\mathbf{r}, \mathbf{R}) = \int d\mathbf{k} e^{i\mathbf{k}\cdot\mathbf{r}} \Delta(\mathbf{k}, \mathbf{R}). \quad (2.4)$$

In the NS interface (at $x=0$) problems, we assume that the superconducting order parameter is not degraded by the normal metal, and thus neglect the proximity effect, i.e.,

$$\Delta(\mathbf{k}, \mathbf{R}) = \Delta(\mathbf{k}) \Theta(x), \quad (2.5)$$

where $\Theta(x)$ is a step function. Investigation of the BdG equations shows that the eigenfunctions (u, v) will oscillate on a length scale k_F^{-1} , the inverse Fermi wave vector, because the pair potential is usually much smaller than the Fermi energy. Thus, the effect of superconductivity on the wave functions is limited to small deviations of the wave vector from k_F . This fast oscillation on the length scale k_F^{-1} does not affect the integration, because the pair potential varies only on a scale much larger, namely the coherence length $\xi_0 (= k_F/2m\Delta_0) \gg k_F^{-1} (= k_F/2mE_F)$. This suggests that we can introduce new wave functions

$$\begin{pmatrix} \bar{u} \\ \bar{v} \end{pmatrix} = e^{-\mathbf{k}_F \cdot \mathbf{x}} \begin{pmatrix} u \\ v \end{pmatrix}, \quad (2.6)$$

in which we divide out the fast oscillations. If we retain only terms of lowest order in $(k_F \xi_0)^{-1}$ (WKB approximation¹⁷), the substitution of (2.6) into (2.2) and (2.3) leads to the Andreev equations,^{16,18}

$$E\bar{u}(\mathbf{x}) = -im^{-1} \mathbf{k}_F \cdot \nabla \bar{u}(\mathbf{x}) + \Delta(\hat{\mathbf{k}}_F, \mathbf{x}) \bar{v}(\mathbf{x}), \quad (2.7)$$

$$E\bar{v}(\mathbf{x}) = im^{-1} \mathbf{k}_F \cdot \nabla \bar{v}(\mathbf{x}) + \Delta(\hat{\mathbf{k}}_F, \mathbf{x}) \bar{u}(\mathbf{x}). \quad (2.8)$$

From now on we assume that the NS interface is lying in the y - z plane and is translationally invariant so that the spatial dependence of \bar{u} , \bar{v} , and Δ is reduced to the dependence only on x . In this case, the Andreev equations (2.7) and (2.8) take the form

$$E\bar{u}(x) = -im^{-1} k_{Fx} \frac{d\bar{u}(x)}{dx} + \Delta(\hat{\mathbf{k}}_F, x) \bar{v}(x), \quad (2.9)$$

$$E\bar{v}(x) = im^{-1} k_{Fx} \frac{d\bar{v}(x)}{dx} + \Delta(\hat{\mathbf{k}}_F, x) \bar{u}(x). \quad (2.10)$$

For $\Delta(\hat{\mathbf{k}}_F, \mathbf{x})$ given by Eq. (2.5), these equations can be solved exactly. For $E > |\Delta|$ [hereafter, we denote $\Delta \equiv \Delta(\mathbf{k})$ for convenience], we find $(\bar{u}, \bar{v}) = e^{ikx} (\tilde{u}, \tilde{v})$, where $k = (m/|k_{Fx}|) \sqrt{E^2 - \Delta^2}$ and $\tilde{u} = \text{sgn}(\Delta) u_0$ and $\tilde{v} = v_0$ with

$$u_0 = \sqrt{[1 + E^{-1}(E^2 - \Delta^2)^{1/2}]/2}, \quad (2.11)$$

$$v_0 = \sqrt{[1 - E^{-1}(E^2 - \Delta^2)^{1/2}]/2}. \quad (2.12)$$

Similarly, for $E < |\Delta|$, we find $k = i(m/|k_{Fx}|)\sqrt{\Delta^2 - E^2}$ and

$$u_0 = \sqrt{[1 + iE^{-1}(\Delta^2 - E^2)^{1/2}]/2}, \quad (2.13)$$

$$v_0 = \sqrt{[1 - iE^{-1}(\Delta^2 - E^2)^{1/2}]/2}. \quad (2.14)$$

III. I - V CHARACTERISTIC OF d_{xy} -NS JUNCTIONS

A. BTK method

In this section, we study the I - V characteristics of a d_{xy} -NS junction shown in Fig. 1 using the Andreev equations (2.9) and (2.10) derived in the previous section. Coherent scattering of quasiparticles, from both the superconducting pair potential $\Delta(x)$ and the ordinary electrostatic potential $V(x)$ due to a thin insulating barrier, produces a wave interference pattern which should be observable experimentally. Introducing such an barrier potential $V(x)$ into a ballistic NS junction will modify the wave interference pattern of the quasiparticles, and should dramatically affect the current-voltage (I - V) characteristics of the junction.^{19,20} BTK demonstrated¹⁵ that a tunnel barrier, located at the NS interface, produces an I - V characteristics which interpolates smoothly between the tunnel junction ($V \neq 0$) and ballistic junction ($V = 0$) limits. We adopt the model and formalism of BTK, but extend the calculation by allowing the tunnel barrier to exist anywhere inside the normal metal for a d_{xy} -NS junction. In this model, we expect that there will exist bound states trapped between the barrier potential and the superconductor, caused by a particle alternately experiencing conventional specular reflections at the barrier and Andreev reflections¹⁸ at the NS interface [see Fig. 2(a)]. The latter is caused by the off-diagonal pair potential, so it changes an electron of wave vector \mathbf{k} into a hole of $-\mathbf{k}$, and vice versa, whereas the former only changes the sign of k_x , without changing the nature of the particle. Let us look at an electron in different scattering processes. In process (1) [see Fig. 2(a)], the electron has a momentum $(+k_x, +k_y)$ and senses a positive pair potential because of $\Delta(\hat{\mathbf{k}}) \propto k_x k_y$. On the other hand, in the next scattering process (2), the momentum of the electron changes to $(-k_x, +k_y)$, so this electron will experience a negative pair potential. A similar argument also holds for a hole in the opposite scattering processes. This implies that the sign of the pair potential sensed by the quasiparticles will reverse at each consecutive Andreev reflection if the superconductor is d_{xy} wave [see Figs. 2(b) and 2(c)]. Such a sign reversal would not occur in an identical model if the superconductor was s -wave like, whether isotropic or anisotropic.

Following BTK, we take $V(x) = V_0 \delta(x+L)$, which represents the potential of the tunnel barrier where $x = -L$ is the position of the barrier. This δ -function potential is accounted for the boundary condition in N and S and can therefore be omitted from the Hamiltonian. In order to calculate the current through the junction, we need the transmission coefficients. We note that the wave functions satisfy the Andreev equations (2.9) and (2.10), in all regions (see Fig. 2), provided that the pair potential is taken to be zero in the normal regions I and II. The general solution to this scattering problem is

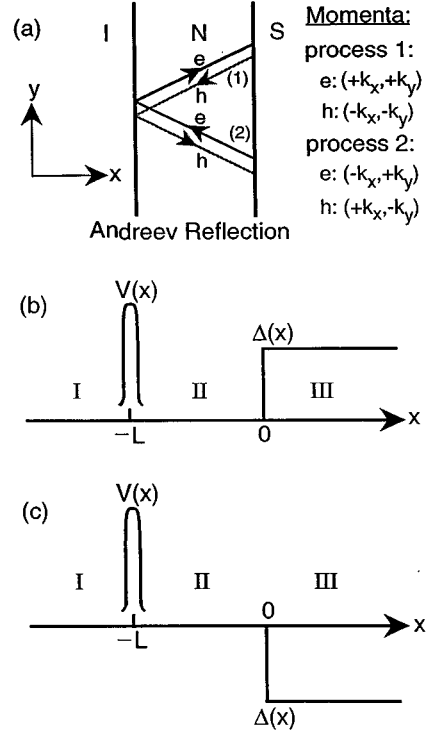


FIG. 2. (a) Andreev reflection in the NS interface and the momentum states of the quasiparticles in different scattering processes. (b) and (c) are plots of barrier potential $V(x) = V\delta(x+L)$ and pair potential $\Delta(x)$. The pair potential sensed by the particle at consecutive Andreev reflections will be alternate in sign, i.e., during one reflection the particle will sense it as a *potential barrier* (b), and the particle will experience it as a *potential well* in next consecutive process (c).

$$\psi_{\text{I}}(x) = \begin{pmatrix} 1 \\ 0 \end{pmatrix} e^{iq_+x} + a \begin{pmatrix} 0 \\ 1 \end{pmatrix} e^{iq_-x} + b \begin{pmatrix} 1 \\ 0 \end{pmatrix} e^{-iq_+x}, \quad (3.1)$$

$$\psi_{\text{II}}(x) = e \begin{pmatrix} 1 \\ 0 \end{pmatrix} e^{iq_+x} + f \begin{pmatrix} 1 \\ 0 \end{pmatrix} e^{-iq_+x} + g \begin{pmatrix} 0 \\ 1 \end{pmatrix} e^{iq_-x} + h \begin{pmatrix} 0 \\ 1 \end{pmatrix} e^{-iq_-x}, \quad (3.2)$$

$$\psi_{\text{III}}(x) = c \begin{pmatrix} u_0 \\ v_0 \end{pmatrix} e^{ik_+x} + d \begin{pmatrix} v_0 \\ -u_0 \end{pmatrix} e^{-ik_-x}, \quad (3.3)$$

with $q_{\pm} = |k_{Fx}| \pm mE/|k_{Fx}|$ and $k_{\pm} = |k_{Fx}| \pm m\sqrt{E^2 - \Delta^2}/|k_{Fx}|$. u_0 and v_0 are defined in Eqs. (2.11)–(2.14). The coefficients a, b, \dots are to be determined from the boundary conditions:

$$\psi_{\text{I}}(-L) = \psi_{\text{II}}(-L), \psi_{\text{II}}(0) = \psi_{\text{III}}(0), \quad (3.4)$$

$$\psi'_{\text{II}}(-L) - \psi'_{\text{I}}(-L) = 2mV_0\psi_{\text{I}}(-L), \psi'_{\text{II}}(0) = \psi'_{\text{III}}(0). \quad (3.5)$$

Because of current continuity, the amplitudes at any fixed x are sufficient to determine the current. Following BTK, we determine the current in the region I, i.e., we only need the coefficients a and b in Eq. (3.1). After some algebra, we find

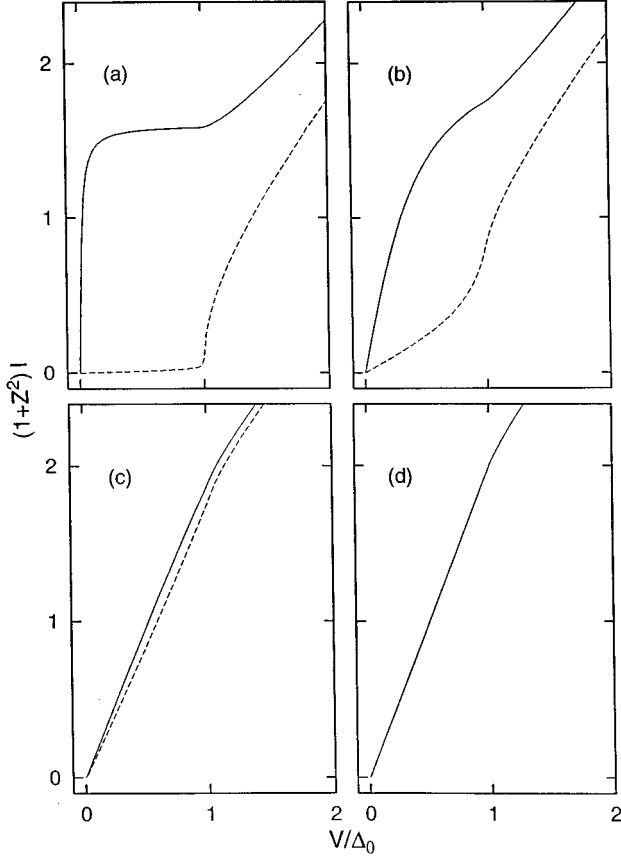


FIG. 3. Current for a d_{xy} -NS junction (solid line) and s -NS junction (dashed line) with $L/\xi_0=0$: (a) $Z=5$, (b) $Z=1$, (c) $Z=0.2$, and (d) $Z=0$. The wave vector of the incoming electron is chosen as $\hat{\mathbf{k}}=(1/\sqrt{2})(1,1,0)$.

$$a = \frac{1}{D} \left(\frac{v_0}{u_0} \right) \left(\frac{1}{1+Z^2} \right), \quad (3.6)$$

$$b = \frac{1}{D} \left(\frac{-iZ}{1+iZ} \right) e^{-2iq_+L} \left[1 + \left(\frac{v_0^2}{u_0^2} \right) e^{2i(q_+ - q_-)L} \right], \quad (3.7)$$

with

$$D = 1 + \left(\frac{Z^2}{1+Z^2} \right) \left(\frac{v_0^2}{u_0^2} \right) e^{2i(q_+ - q_-)L}, \quad (3.8)$$

where $Z=(k_F/|k_{Fx}|)Z_0$ with $Z_0=mV/k_F$ being the dimensionless barrier strength.

B. I - V characteristics

Using the coefficients a and b obtained in the previous section, we are able to calculate the I - V relationship of the d_{xy} -NS junction:¹⁵

$$I = \frac{e}{\pi} \int_{-\infty}^{\infty} dE [f(E-eV) - f(E)] [1 + |a(E)|^2 - |b(E)|^2], \quad (3.9)$$

where $f(E)$ is the Fermi distribution function. We note that the current I in Eq. (3.9) depends on the wave vector of the incoming electrons. Figure 3 shows the I - V relationship at

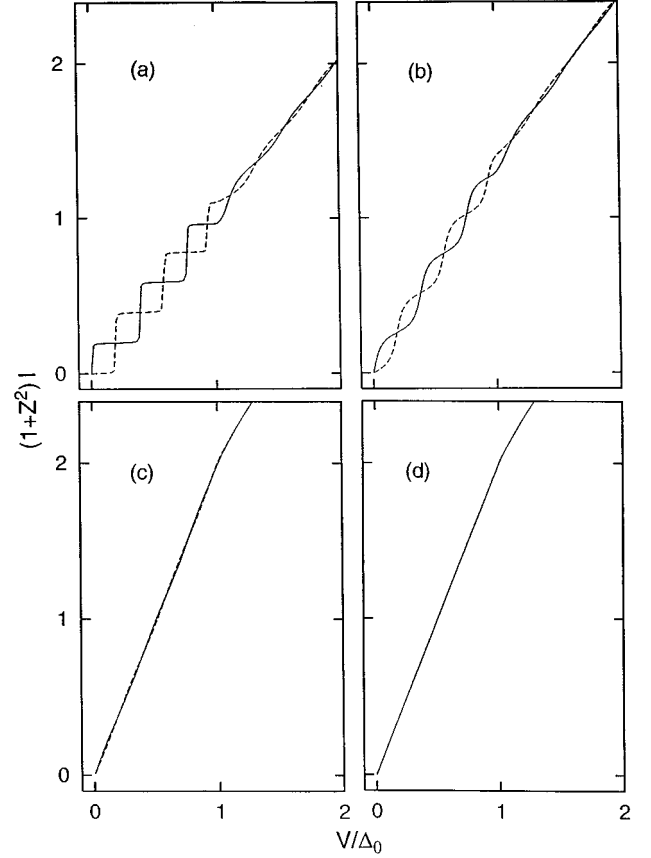


FIG. 4. Same as in Fig. 3 but with $L/\xi_0=5$.

$L=0$ from Eq. (3.9) for the incoming electrons with a single wave vector $\hat{\mathbf{k}}=(1/\sqrt{2})(1,1,0)$. The current for a conventional s -wave NS junction is also shown in the figure for comparison. It is clear that the usual I - V behavior for an s -NS tunnel junction (Z large) is obtained when the barrier is located at the NS interface ($L=0$). Figure 4 shows the result for the current as we move the barrier away from the NS interface ($L/\xi_0=5$). It can be seen that additional sharp current steps appear. These current steps arise from bound states trapped between the barrier and the superconductor. However, the positions of the current steps in the d_{xy} -NS junction are found to be exactly out of phase relative to those in the s -NS junction. In particular, a zero-energy step, which does not depend on L , always exists in the d_{xy} -NS junction. We note from Figs. 3 and 4 that the difference between d_{xy} - and s -NS junctions can be observed in the I - V curve, not only when a tunnel barrier is present, where Z is large, but also in the ballistic case (Z small), except when $Z \rightarrow 0$, where the I - V characteristics of s - and d_{xy} -NS junctions become indistinguishable.

Figure 5 shows plots of conductance $G=dI/dV$ at $L=0$ for several junctions with different values of Z . It can be seen that, in the tunnel junction limit [large Z , see Fig. 5(a)], a sharp subgap transmission resonance, corresponding to the steps in current shown in Fig. 3(a), appear in the conductance of a d_{xy} -NS junction. Figure 6 shows the conductance for $L/\xi_0=5$. We see that more subgap resonances appear in G . The positions of these subgap resonances in the d_{xy} -NS junction are also exactly out of phase relative to those in the

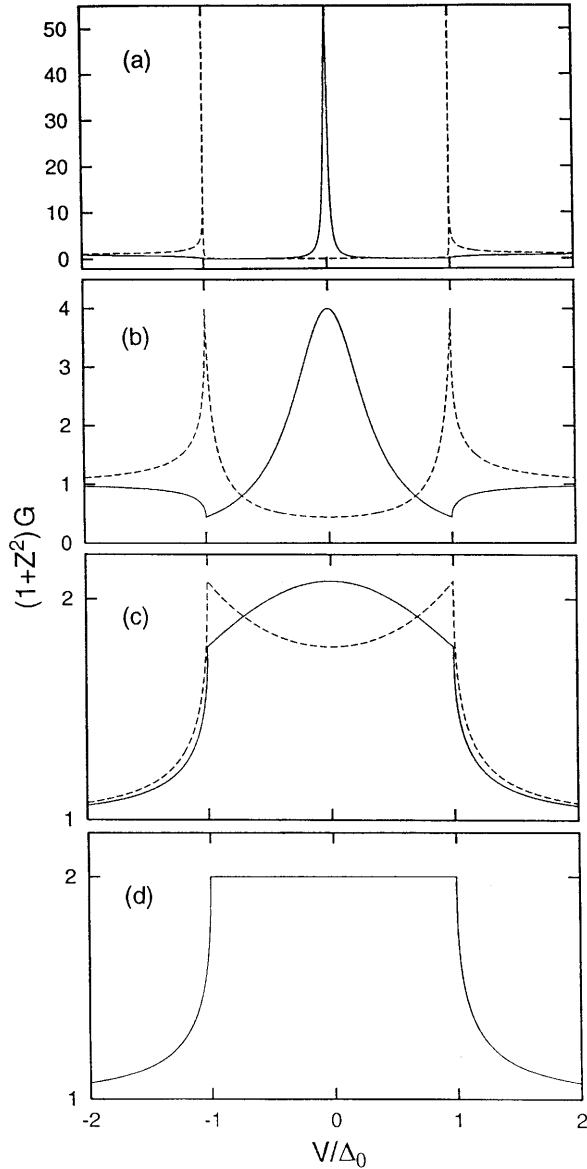


FIG. 5. Differential conductance for a d_{xy} -NS junction (solid line) and s -NS junction (dashed line) with $L/\xi_0=0$: (a) $Z=5$, (b) $Z=1$, (c) $Z=0.2$, and (d) $Z=0$. The wave vector of the incoming electron is chosen as $\hat{\mathbf{k}}=(1/\sqrt{2})(1,1,0)$.

s -NS junction. In particular, a midgap resonance at zero voltage, corresponding to the ZBA, is obtained for the d_{xy} -NS junction. As Z decreases, the number and positions of the resonances remain unchanged, except that the peaks become broader. In particular, in the ballistic limit ($Z=0$), the conductance of a d_{xy} -NS junction becomes identical to that of an s -NS junction.

In fact, the steps in the I - V curves (Figs. 3 and 4), and the subgap resonances in the conductance (Figs. 5 and 6) are direct consequences of the bound states formed inside the energy gap. These bound states are defined as poles of the current transmission amplitude. Setting $D=0$ in Eq. (3.8) determines these poles and therefore the bound states:

$$\left(\frac{Z^2}{1+Z^2}\right)\left(\frac{v_0^2}{u_0^2}\right)e^{2i(q_+-q_-)L}=-1. \quad (3.10)$$

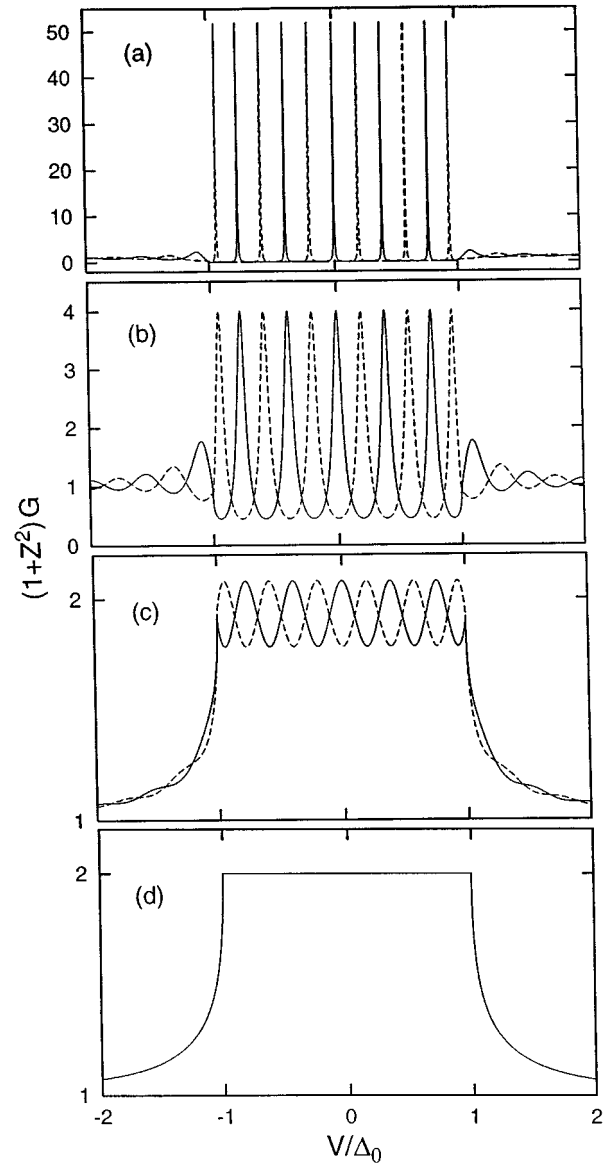


FIG. 6. Same as in Fig. 5 but with $L/\xi_0=5$.

A complex energy $E=E_R+iE_I$ is required to solve Eq. (3.10), where E_R is the energy of the resonance and $1/|E_I|$ is its lifetime. The resonances are well described by Eq. (3.10), which gives the positions E_R of the bound levels:

$$\begin{aligned} (E_R/\Delta_0)(k_F/|k_{Fx}|)-(\xi_0/L)\cos^{-1}(E_R/|\Delta|) \\ = \begin{cases} (n+1/2)\pi\xi_0/L & \text{for a } d_{xy}\text{-NS junction,} \\ n\pi\xi_0/L & \text{for an } s\text{-NS junction,} \end{cases} \end{aligned} \quad (3.11)$$

where $n=0,\pm 1,\dots$. While the leakage rate $2E_I$ is approximately given by

$$2E_I \approx \frac{\xi_0|\Delta|}{L} \ln\left(\frac{Z^2}{1+Z^2}\right). \quad (3.12)$$

Note that $E_I<0$, as required for a system to be stable. Equation (3.11) is similar to the condition for Andreev bound levels in a SNS junction,²¹ except that the Andreev bound

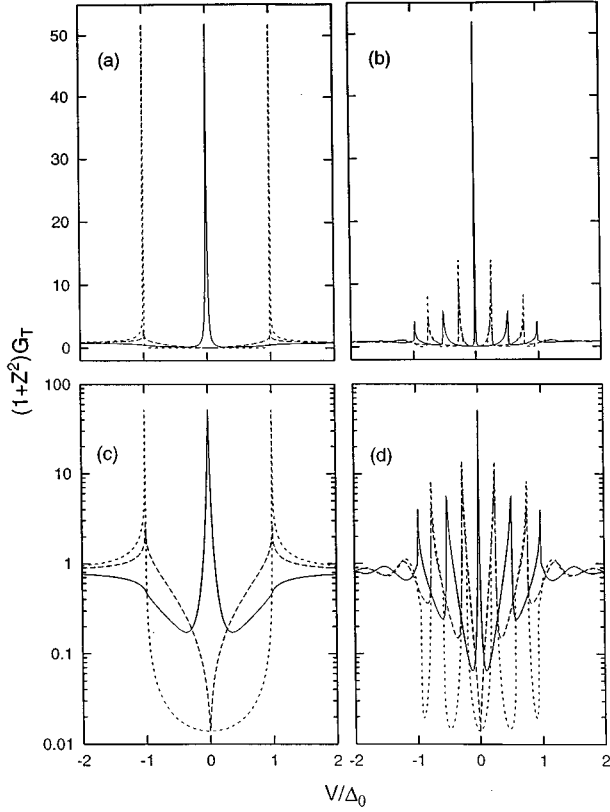


FIG. 7. G_T for a d_{xy} -NS junction (solid line), anisotropic s -NS junction with order parameter $\Delta_s(\hat{\mathbf{k}}) = 2\Delta_0|\hat{k}_x\hat{k}_y|$ (dashed line), and isotropic s -NS junction (dotted line) with $Z=5$: (a) $L/\xi_0=0$ and (b) $L/\xi_0=5$. (c) and (d) are semilogarithmic plots of (a) and (b), respectively.

levels in the NS junctions are leaky. The width of the transmission resonances is limited by the partial leakage through the barrier potential, so the resonance lifetime is approximately $1/2|E_I|$.

It is also clear from Eq. (3.11) that, for large L , additional resonances appear — approximately one new resonance for each ξ_0 increase in L if the wave vector of the incoming electron is neither nearly parallel nor perpendicular to the interface. In particular, there always exists a zero-energy solution ($E_R=0$) for the d_{xy} -NS junction from Eq. (3.11), but not for the s -NS junction. This zero-energy solution should correspond to the midgap state discussed in Ref. 12. More remarkably, we find that if $L < \xi_0$ for an s -NS junction, the lowest energy bound state occurs at the gap edge ($E=\Delta$), and no bound states exist inside the energy gap. In a d_{xy} -NS junction, however, the zero-energy step in the current or zero-energy resonance in the conductance always exists even when $L \rightarrow 0$. This can be clearly seen from the results presented in Figs. 5 and 6 for junctions with different L .

The above discussion is for incoming electrons with a single $\hat{\mathbf{k}}$ direction. If a convolution of all possible $\hat{\mathbf{k}}$ directions is considered, the current is then given by $I_T = \sum_{\hat{\mathbf{k}}} P(\hat{\mathbf{k}}) I(\hat{\mathbf{k}})$ with $P(\hat{\mathbf{k}})$ being the probability of incoming electrons with wave vector $\hat{\mathbf{k}}$. Figures 7(a) and 7(b) show $G_T = dI_T/dV$ at large Z ($=5$) for a d_{xy} -NS junction (solid

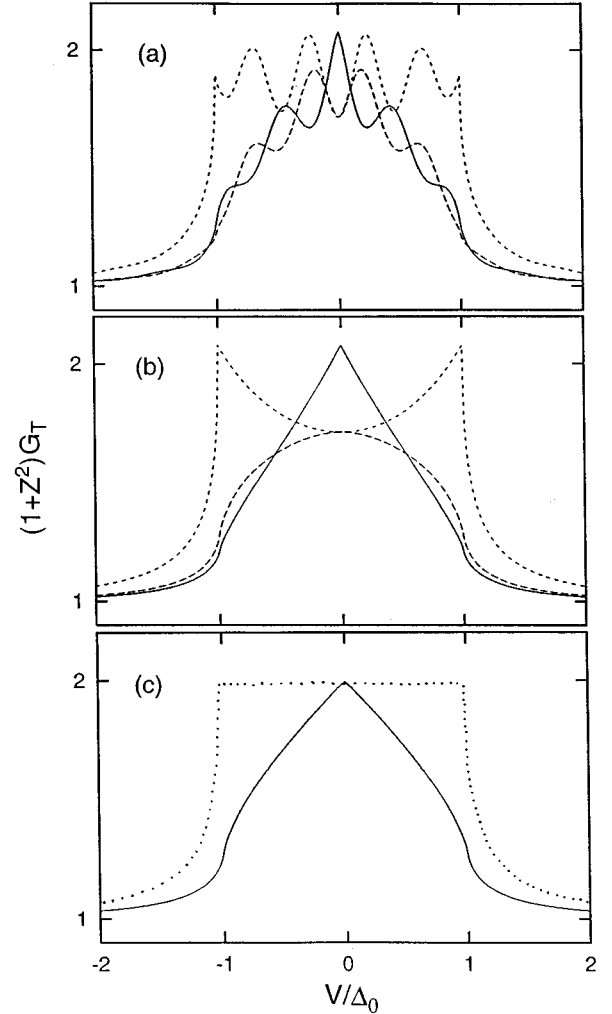


FIG. 8. G_T for a d_{xy} -NS junction (solid line), anisotropic s -NS junction with order parameter $\Delta_s(\hat{\mathbf{k}}) = 2\Delta_0|\hat{k}_x\hat{k}_y|$ (dashed line), and isotropic s -NS junction (dotted line) with (a) $Z=0.2$, $L/\xi_0=5$; (b) $Z=0.2$, $L/\xi_0=0$; and (c) $Z=0$.

line), an anisotropic s -NS junction with $\Delta_s(\hat{\mathbf{k}}) = 2\Delta_0|\hat{k}_x\hat{k}_y|$ (dashed line), and an isotropic s -NS junction (dotted line). Here we have taken $P(\hat{\mathbf{k}}) = 1$. We see from the figure that most of the resonances are strongly suppressed. However, the zero-energy resonance, corresponding to the ZBA, in the d_{xy} -NS junction remains quite pronounced. This result is expected since the positions of the resonances at nonzero energies are different for different $\hat{\mathbf{k}}$, whereas the conductance in the d -NS junction for any $\hat{\mathbf{k}}$ has a zero-energy resonance. Consequently, the resonances of G_T at nonzero energies are suppressed, while the zero-energy resonance is enhanced. In order to more clearly see the states inside the energy gap, we replot G_T for $Z=5$ on a semilog scale in Figs. 7(c) and 7(d). Figure 8 is the result for G_T in the small Z limit. We see that, even when $Z=0.2$ [Figs. 8(a) and 8(b)], there still exists a difference in between conductances of s - and d_{xy} -NS junctions. However, in the ballistic limit ($Z=0$) [Fig. 8(c)], the results of a d_{xy} - and anisotropic s -NS junctions, which are independent of L , become identical, while the isotropic s -NS junction still shows a different I - V characteristic.

C. Comparison with experiments

The above calculations show that conductance resonance of the conductance at zero energy for a d_{xy} -NS junction should be much easier to observe than the other resonances or than the resonances in an s -NS junction, since the midgap state is insensitive to the junction parameters. Scanning tunneling microscopy measurements have been performed on a normal metal droplet on an s -wave low- T_c superconductor,²² and weak resonances in G have already been observed. Moreover, numerous ZBA's, similar to those predicted in Figs. 7 and 8, have been observed in the conductances of normal metal contacts and quasiparticle (e.g., point contact) tunnel junctions on high- T_c superconductors, although none of the samples studied have perfect $\{110\}$ surfaces.^{11,13} However, a $\{110\}$ surface is not a necessary condition to observe ZBA's in a $d_{x_a^2-x_b^2}$ -wave superconductor. Any $d_{x_a^2-x_b^2}$ -wave NS junction, whose interface has an arbitrary tilt angle α relative to the crystal axis, has the possibility for the zero-energy state to exist, since the incoming electrons with wave vectors within the ranges $\pm\pi/4 - \alpha < \tan^{-1}(k_y/k_x) < \pm\pi/4 + \alpha$ will experience an odd off-diagonal potential. Alternatively, simple off-axis tunneling should yield a d_{xy} component. This might explain why the ZBA is such a ubiquitous phenomenon in high- T_c superconductors.²³

In the past several years, there have been a number of tunneling studies on both single crystalline and ceramic high- T_c superconducting oxides using point-contact measurements.¹⁰ The experimental data have often been fit using the BTK model. The fits are generally satisfactory, except for the inability of the model to readily explain the ZBA and resonance peaks within the framework of s -wave pairing symmetry. On the other hand, these anomalies in the tunneling data can be consistently explained if we assume that high- T_c superconductors have d -wave pairing symmetry. Consider a tunneling process along the a axis in the ab planes of high- T_c materials. In the presence of a $\{110\}$ -surface component, the tunneling conductance will approximately be given by the sum of the contributions from the $\{100\}$ - and $\{110\}$ -surfaces:

$$\tilde{G}_T = \gamma G_T^{\{110\}} + (1 - \gamma) G_T^{\{100\}}, \quad (3.13)$$

where $0 \leq \gamma \leq 1$ represents the weight of the contribution from the $\{110\}$ surface. Figure 9 depicts the calculated differential conductance at $Z=1$ for different values of γ . For $\gamma=0$, the \tilde{G}_T - V curve corresponds to the result of a $d_{x^2-y^2}$ -NS junction along the a direction, i.e., without ZBA, which is indistinguishable from that of an anisotropic s -NS junction with $\Delta(\mathbf{k}) = \Delta_0 |\hat{k}_x^2 - \hat{k}_y^2|$. As γ increases, the contribution of $\{110\}$ surface becomes more important and the ZBA at zero voltage is enhanced. The results for large Z ($=5$) are shown in Fig. 10. We see that even a small $\{110\}$ -surface component is enough to cause a significant zero-voltage peak. Thus, using our results, one can readily explain why the ZBA is so frequently observed in high- T_c superconductors. Nevertheless, it is preferable to use samples with ideal $\{110\}$ surfaces to unambiguously confirm the existence of such a zero-bias resonance.

For the heavy-fermion superconductor URu₂Si₂, it has been argued,^{8,9} based on the data of specific heat and point-

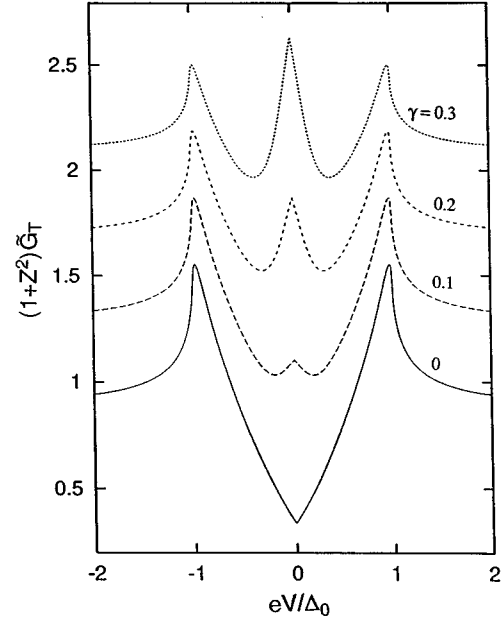


FIG. 9. Conductance for a d -wave NS junction with different $\{110\}$ -surface component at $L=0$ and $Z=1$.

contact spectroscopy, that the pairing state of URu₂Si₂ has d_{xy} -wave symmetry. However, we note that the point-contact data was essentially taken in the ballistic limit ($Z=0$), as fit by the authors of Refs. 8 and 9 using the BTK model. As we have shown previously, in this limit, a d_{xy} -wave gap function ($\sim k_x k_y$) and anisotropic s -wave gap function ($\sim |k_x k_y|$) give rise to exactly the same I - V characteristics (see Fig. 8(c)). More precisely, in the limit of $Z \sim 0$, isotropic s -wave BTK theory predicts a conductance peak with a flat top. However, both d -wave and anisotropic s -wave order parameters permit low-energy excitations at the nodes in the gap, so that their BTK conductance characteristics near zero bias

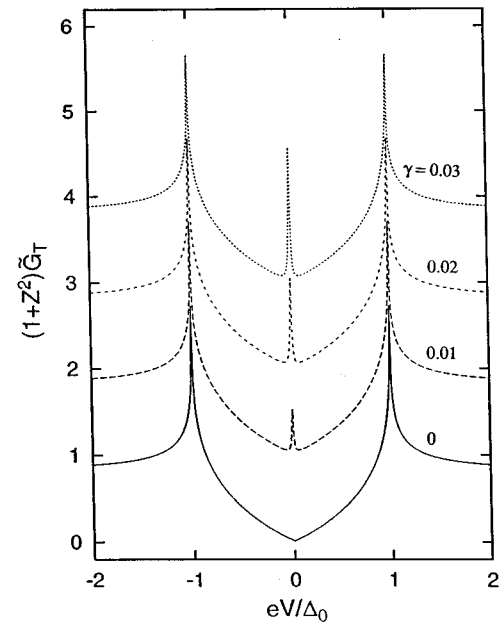


FIG. 10. Same as in Fig. 9 but at $Z=5$.

have more of a triangular shape. In addition, the specific heat depends only on the vanishing energy gap for certain directions in k space, and not on the sign of the order parameter. Thus, in principle, the experimental data on specific heat and the point-contact spectroscopy measurements at $Z \sim 0$ can also be interpreted in terms of an anisotropic s -wave pairing state. Thus, in order to clearly determine the pairing state of URu₂Si₂, it is preferable to do point-contact measurements in the tunnel barrier limit (large Z).

IV. DISCUSSION AND CONCLUSIONS

We have studied the I - V characteristics of a d -wave NS junction with a special geometry using the BdG equations. Such a junction allows one to directly examine the consequences of the sign change of a $d_{x^2-y^2}$ -wave order parameter. The so-called d_{xy} -NS junction, formed by normal metal in contact with a d_{xy} -wave superconductor (e.g., the heavy-fermion superconductor URu₂Si₂) with a $\{100\}$ surface, or with a $d_{x^2-y^2}$ -wave superconductor (e.g., a high- T_c superconductor) with a $\{110\}$ surface, has been carefully studied. We have shown that there exist bound states inside the energy gap trapped between the tunnel barrier and the superconductor. These bound states cause steps in the I - V curve and subgap resonances in the differential conductance, the positions of which have been found to be exactly out of phase relative to those observed in conventional s -NS junctions. In particular, a zero-voltage step in the I - V characteristic and a resonance in the conductance, or ZBA, has been obtained for the d_{xy} -NS junction. We have used these results to analyze some experimental point-contact tunneling spectroscopy data obtained from high- T_c superconductors and the heavy-fermion superconductor URu₂Si₂. We have pointed out that, in numerous tunneling spectroscopy measurements performed on high- T_c superconductors, ZBA's, similar to our predictions in Figs. 9 and 10, have often been observed, although none of the samples used have a perfect $\{110\}$ surface. This puzzle can be consistently solved if we assume that the high- T_c superconductors have a $d_{x^2-y^2}$ -wave pairing state, since we have shown that even a few percent $\{110\}$ -surface component in a $\{100\}$ -NS junction is sufficient to cause a sizable zero-voltage peak. Thus, using our results, one can readily explain ZBA's are so frequently observed in high- T_c superconductors. For the heavy-fermion superconductor URu₂Si₂, we pointed out that available specific-heat and point-contact data in the ballistic limit ($Z \sim 0$) are not sufficient to determine the pairing symmetry. In order to cleanly confirm the pairing state in URu₂Si₂, it is preferable to do point-contact measurements in the tunnel barrier limit.

The zero-bias anomaly (see Figs. 3 and 5) studied in the present paper has also been investigated by Tanaka *et al.*^{24,25} using a similar method. The case they discussed corresponds to $L=0$ in Fig. 2, or the barrier potential touching the surface of the superconductor. On the other hand, we consider both $L=0$ and $L \neq 0$ cases. For $L \neq 0$, in addition to the zero-bias anomaly, several resonating states inside the gap were also predicted (see Figs. 4, and 6–8). The positions of these resonances should provide an important clue to the pairing symmetry of the superconductor. Furthermore we also studied how robust the ZBA is, if the surface of the $d_{x^2-y^2}$ -wave superconductor is not completely along the $\{110\}$ direction (see Figs. 9 and 10).

Several alternative explanations for ZBA's in high- T_c superconducting tunnel junctions have also been proposed in the literature (see Ref. 13 and the references therein) within the framework of s -wave pairing. Such explanations include local magnetic states on the superconducting surface, a peak in the electron density of states near the Fermi energy, etc., however, one can readily distinguish our proposed mechanism from other possible mechanisms. If the observed ZBA is indeed due to d_{xy} symmetry, it must possess the following signatures: (a) by increasing γ (see Figs. 9 and 10), the weight of ZBA in the differential conductance should become greatly enhanced, and (b) for $L \neq 0$, weak equally spaced resonances, in addition to the ZBA, should appear [see Figs. 7(b) and 8(a)]. These features are unique to a d_{xy} (or $d_{x^2-y^2}$ with a $\{110\}$ -oriented surface) superconductor and still need to be confirmed by experimental measurements. Finally, it is necessary to point out that in our calculations, the proximity effect, i.e., the self-consistent condition for the order parameter, has been neglected. As argued by the author of Ref. 12, even when this effect is taken into account, the midgap state still exists. Thus we expect that the transport anomalies predicted for the d_{xy} -NS junction will survive. Since these anomalies are intrinsic in nature and are generated by the sign change of the off-diagonal potential, the essential features of the conductance discussed in the present paper should not depend on the detailed structure of the pair potential.

ACKNOWLEDGMENTS

We thank Professor C. R. Hu for useful discussions. This research was supported by the Robert A. Welch Foundation, and by the State of Texas through the Texas Center for Superconductivity at University of Houston, the Advanced Research Program, and the Advanced Technology Program.

¹N. E. Bickers, D. J. Scalapino, and R. T. Scalettar, Int. J. Mod. Phys. B **1**, 687 (1987); Z. Y. Weng, T. K. Lee, and C. S. Ting, Phys. Rev. B **38**, 6561 (1988); P. Mouthoux, A. V. Balatsky, and D. Pines, Phys. Rev. Lett. **67**, 3448 (1991).

²W. N. Hardy, D. A. Bonn, D. C. Morgan, R. Liang, and K. Zhang, Phys. Rev. Lett. **70**, 3999 (1993).

³Z. X. Shen, D. S. Dessau, B. O. Wells, D. M. King, W. E. Spicer, A. J. Arko, D. Marshall, L. W. Lombardo, A. Kapitulnik, P.

Dickinson, S. Doniach, J. DiCarlo, A. G. Loeser, and C. H. Park, Phys. Rev. Lett. **70**, 1553 (1993).

⁴D. A. Wollman, D. J. Van Harlingen, W. C. Lee, D. M. Ginsberg, and A. J. Leggett, Phys. Rev. Lett. **71**, 2134 (1993); D. A. Wollman, D. J. Van Harlingen, J. Giapintzakis, and D. M. Ginsberg, Phys. Rev. Lett. **74**, 797 (1995).

⁵A. Mathai, Y. Gim, R. C. Black, A. Amar, and F. C. Wellstoo, Phys. Rev. Lett. **74**, 4523 (1995).

- ⁶C. C. Tsuei, J. R. Kirtley, C. C. Chi, L. S. Yu-Jahnes, A. Gupta, T. Shaw, J. Z. Sun, and M. B. Ketchen, *Phys. Rev. Lett.* **73**, 593 (1994).
- ⁷J. H. Miller, Jr., Q. Y. Ying, Z. G. Zou, N. Q. Fan, J. H. Xu, M. F. Davis, and J. C. Wolfe, *Phys. Rev. Lett.* **74**, 2347 (1995).
- ⁸K. Hasselbach, J. R. Kirtley, and P. Lejay, *Phys. Rev. B* **46**, 5826 (1992).
- ⁹K. Hasselbach, J. R. Kirtley, and J. Flouquet, *Phys. Rev. B* **47**, 509 (1993).
- ¹⁰H. Srikanth and A. K. Raychaudhuri, *Physica C* **190**, 229 (1992).
- ¹¹J. Lesueur, L. H. Greene, W. L. Feldmann, and A. Inam, *Physica C* **191**, 325 (1992).
- ¹²C. R. Hu, *Phys. Rev. Lett.* **72**, 1526 (1994).
- ¹³T. Walsh, *Int. J. Mod. Phys. B* **6**, 125 (1992).
- ¹⁴P. G. de Gennes, *Superconductivity of Metals and Alloys* (Benjamin, New York, 1966).
- ¹⁵G. E. Blonder, M. Tinkham, and T. M. Klapwijk, *Phys. Rev. B* **25**, 4515 (1982).
- ¹⁶C. Bruder, *Phys. Rev. B* **41**, 4017 (1990).
- ¹⁷J. Bardeen *et al.*, *Phys. Rev.* **187**, 556 (1969).
- ¹⁸A. F. Andreev, *Zh. Éksp. Teor. Fiz.* **46**, 1823 (1964) [*Sov. Phys. JETP* **19**, 1228 (1964)].
- ¹⁹R. A. Riedel and P. F. Bagwell, *Phys. Rev. B* **48**, 15 198 (1993).
- ²⁰P. G. de Gennes and D. Saint-James, *Phys. Lett.* **4**, 151 (1963).
- ²¹P. F. Bagwell, *Phys. Rev. B* **46**, 12 573 (1992).
- ²²S. H. Tessmer, D. J. Van Harlingen, and J. W. Lyding, *Phys. Rev. Lett.* **70**, 3135 (1993).
- ²³S. C. Sanders, S. E. Russek, C. C. Clickner, and J. W. Ekin, *Appl. Phys. Lett.* **65**, 2232 (1994).
- ²⁴S. Kashiwaya, Y. Tanaka, M. Koyanagi, H. Takashima, and K. Kajimura, *Phys. Rev. B* **51**, 1350 (1995).
- ²⁵Y. Tanaka and S. Kashiwaya, *Phys. Rev. Lett.* **74**, 3451 (1995).